Available online at www.derpharmachemica.com

ISSN 0975-413X
CODEN (USA): PCHHAX

Der Pharma Chemica, 2016, 8(4):137-154
(http://derpharmachemica.com/archive.html)

QSAR Analysis of Anticancer Activity of Indolin Derivatives as Vascular Endothelial Growth Factor Receptor (VEGFR-2) Inhibitors

Siddharth J. Modi and Vithal M. Kulkarni*

Department of Pharmaceutical Chemistry, Poona College of Pharmacy, Bharati Vidyapeeth University, Pune-411038, Maharashtra, India

---

ABSTRACT

A series of indolin derivatives as anticancer agent was examined to determine the structural requirement of vascular endothelial growth factor receptor (VEGFR-2) inhibition by three-dimensional quantitative structural activity relationship (3D-QSAR) using comparative molecular field analysis (CoMFA) and comparative molecular similarity indices analysis (CoMSIA) methods. Evaluation of 31 compounds (training set) served to established model, which was validated by evaluation of a set of 13 compounds (test set). The lowest energy conformer of a most active molecule obtained from the systematic search was used as the template structure for alignment of data set. The optimum partial least square analysis (PLS) for CoMFA and CoMSIA models exhibited good 'leave-one-out' cross-validated coefficient (q^2) of 0.758 and 0.805, the coefficient of determination (r^2) of 0.950 and 0.934 and good predictive power of (r^2 pred) of 0.885 and 0.861 respectively. The final model of QSAR along with information assembled from contour maps may be used for designing novel indolin derivatives as potent anticancer agents.

Keywords: 3D-QSAR; CoMFA; CoMSIA; VEGFR-2; Indolin derivatives.

INTRODUCTION

After over half a century of chemotherapy research, cancer remains one of the most difficult life-threatening diseases to treat [1]. Extensive studies on cancer suggest that tyrosine kinase receptor play important role in regulating cancer. Vascular endothelial growth factor receptor is a type of membrane receptor tyrosine kinase [2-3]. The membrane receptor tyrosine kinase involved in tumorigenesis which consist of epidermal cell growth factor receptor (EGFR) tyrosine kinase, and vascular endothelial growth factor receptor (VEGFR) tyrosine kinase [4-5].When drug binds to the tyrosine kinase receptor it will be dimerize or couple with the cytoplasm kinase and activate it. after the activation of receptor tyrosine kinase domains phosphorylate the C terminal tyrosine residues, named as autophosphorylation, after that a subsequent phosphorylating activation process occurs called a kinase cascade which results in the amplification of the signal. Proliferation, division, adhesion, morphogenesis, angiogenesis, metastasis and antiapoptosis of cells such cellular process occurs due to phosphorylation of proteins. So,inhibition of Tyrosine kinase will result in the suppression of cell activity related to endothelial growth factor receptor leads to anticancer activity [6].

Currently, large number of VEGFR-2 kinase inhibitors are developed as anticancer agents consisting mainly pyridazine, indoline ketone, quinoline, quinazoline nucleus etc. while, large number of drugs are approved including sorafenib, sunitinib, axitinib, vandetanib, pazopanib etc. [7-11].

A series of indolin derivatives with potent and selective inhibitory activity against EGFR-2/KDR receptor has been reported [12]. In order to derive correlation between the structure and inhibitory activity of these inhibitors, we performed a three-dimensional quantitative structure activity relationship (3D-QSAR) study using comparative molecular field analysis, (CoMFA) and comparative molecular similarity indices analysis (CoMSIA).

3D-QSAR is a wide term including every one of those QSAR techniques which relate perceptible target properties with processed particle based descriptors obtains from the spatial (3dimensional) representation of the atomic structures. This technique has advanced as a characteristic expansion to the established QSAR methodologies spearheaded by Hansch and Free-Wilson and others [13].

CoMFA is utilized to determine the correlation between steric and electrostatic fields of compounds and their biological activity [14]. The CoMFA is applied to a set of compounds which show biological activity with same mechanism. At each part of the molecule and at a probe atom the steric and the electrostatic interaction energies calculated [15].

CoMSIA method was introduced by Klebe et al in 1994, which considers hydrogen bond donor, hydrogen bond acceptor and hydrophobic descriptors, in addition to steric and electrostatic features. To calculate similarity indices in CoMSIA, a probe atom is utilized at regular spaced grid points for the aligned compounds and Gaussian function is used for evaluation of field so, no arbitary definition of cut-off limits. Partial Least Square method is utilized to determine cross-validated r^2 (r^2cv) and conventional r^2 values [16-17].

In this paper, 3D-QSAR studies using CoMFA and CoMSIA methods are applied to generate quantitative models and to specify the region where modification can be carried out to improve the inhibitory activity of compounds. The predictive ability of generated model was validated by external validation method. The model was further accessed to generate contour maps for providing information regarding the interaction of compounds and study the structure activity relationship.

MATERIALS AND METHODS

Datasets

A set of 44 indolin derivatives reported as tyrosine kinase inhibitors were taken from literature for this study [12]. Using the 'create set and random method' option in QSAR project of SYBYL-X 2.0, the compounds were divided arbitrarily into a training set of 31 compounds (70%) and a test set of 13 compounds (30%) [18-20]. Training set and test set were used to generate 3D-QSAR models and validation of generated models. The activity of compounds were assessed with IC values i.e. IC_{50} (nM) which was converted into pIc50(-logIC50). Using Partial Least Square regression analysis the logarithmic affiliation aids to obtain symmetrically distributed data [21]. The Structure of indolin derivatives and its inhibitory activity data are specified in Table 1.

Alignment and Molecular modeling

In the study of 3D-QSAR, alignment is one of the most important steps. There are various alignment techniques in which molecules are aligned with comparable orientation and space conformation. SYBYL-X 2.0 (Tripos Associates Inc, St Louis, Mo, USA) was utilized to perform all the molecular modeling study. Sketch function was used to design the 3D structure and subsequently Gasteiger-Huckel charges applied to all compounds. Energy minimization was performed using the Standard tripos molecular mechanism force field. Here, the distill alignment function was performed [22]. The compound 44 having the highest activity was selected as template for alignment in the data set. Therefore, all the conformers were superimposed on each other and the common core structure formed which has been represented in Figure 1. All the molecules are aligned and represented in Figure 2.

Table 1. Indolin derivatives (1-44) used for training and test sets

Compound no	Compound	VEGFR-2/ KDR inhibitory activity (nM)	pIC_{50}
1*	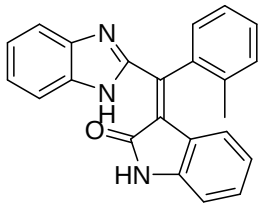	97	7.013
2	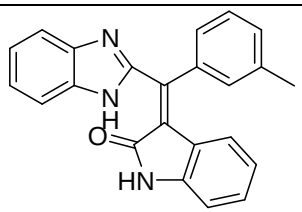	119	6.924
3	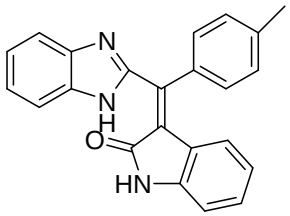	88	7.055
4*	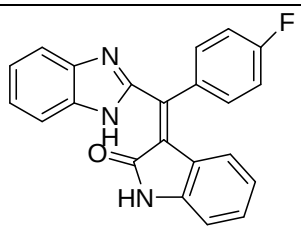	633	6.198
5	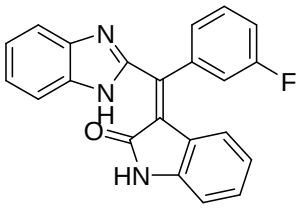	125	6.903
6	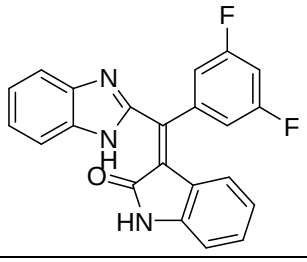	106	6.974
7	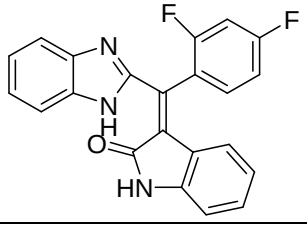	290	6.537

8*	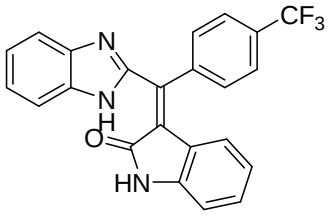	19903	4.701
9*	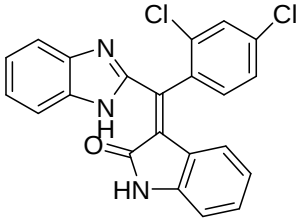	2180	5.661
10	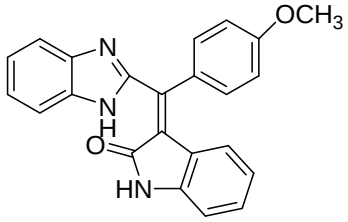	327	6.485
11*	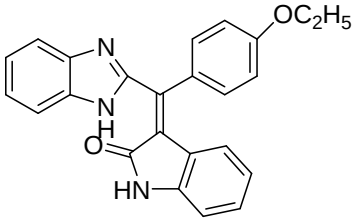	9876	5.000
12	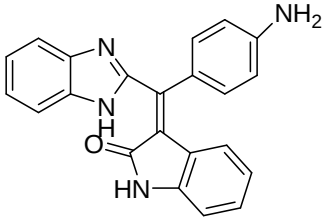	68	7.162
13	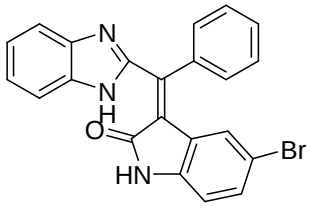	51	7.292
14	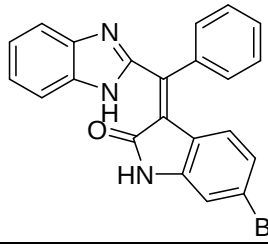	4880	5.311

15	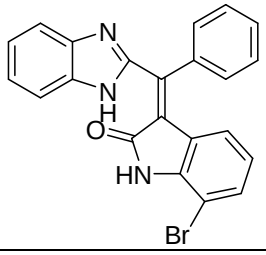	4880	5.311
16	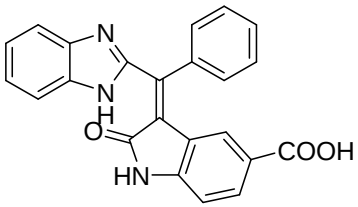	4	8.397
17	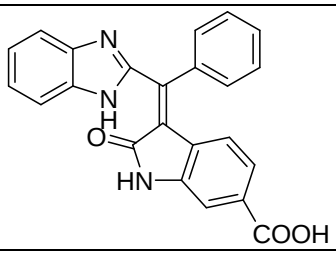	213	6.671
18	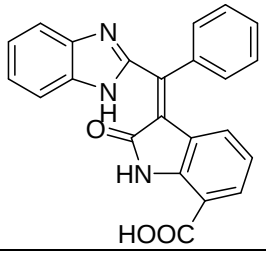	23633	4.626
19	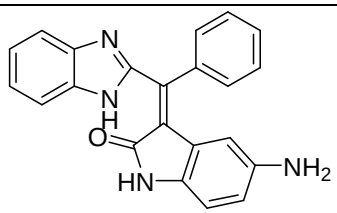	32	7.494
20	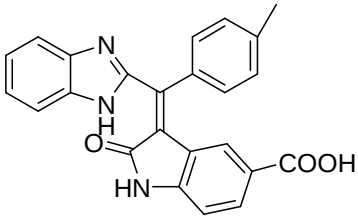	5	8.301
21	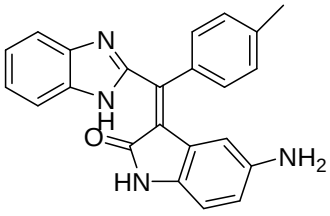	82	7.086

22*	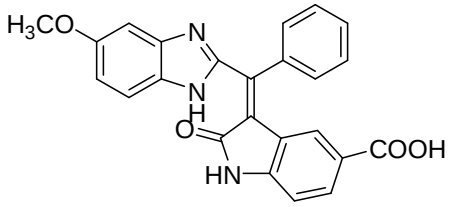	3	8.522
23	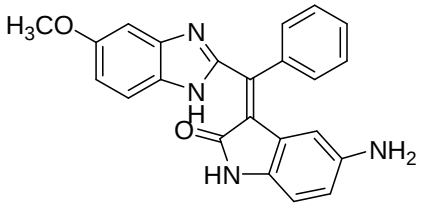	60	7.221
24	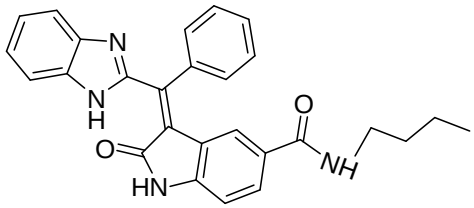	15	7.823
25	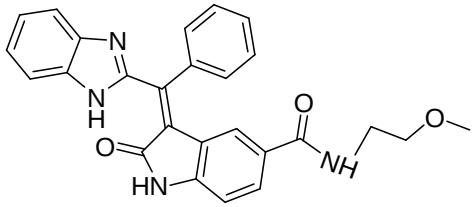	69	7.161
26	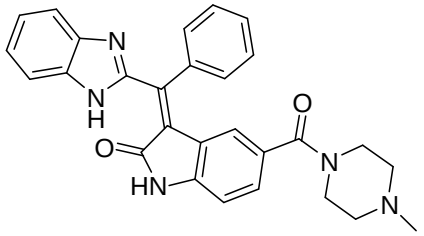	157	6.804
27*	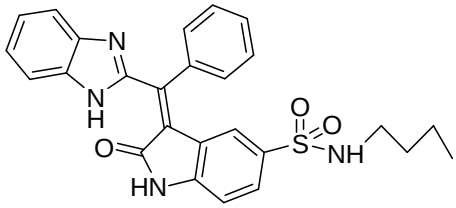	1134	5.945
28*	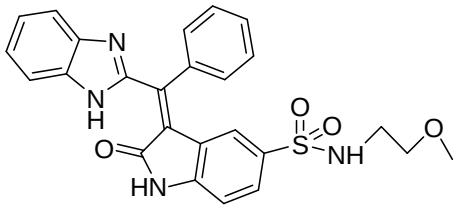	660	6.180

29	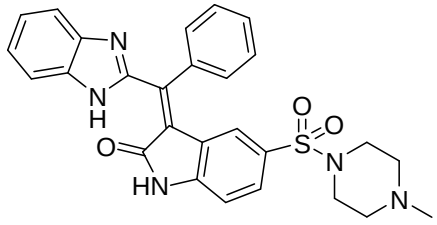	1950	5709
30*	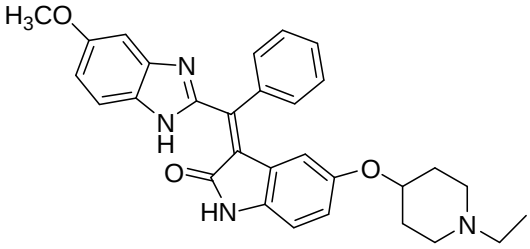	22	7.657
31	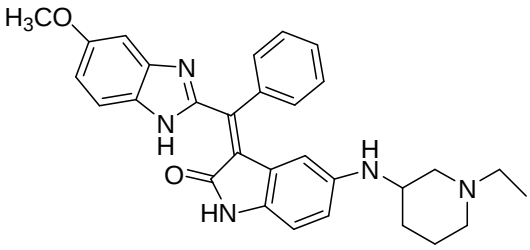	279	6.560
32	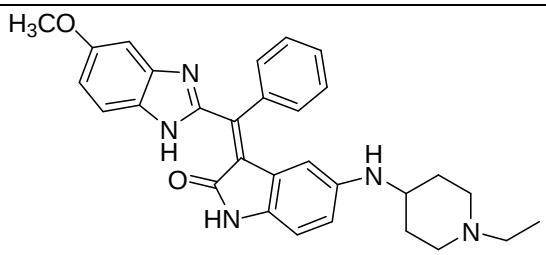	10	8.000
33	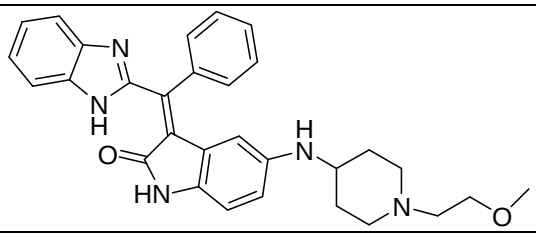	9	8.095
34*	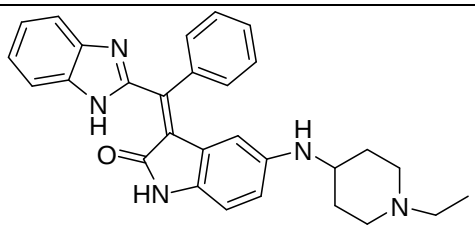	6	8.221
35	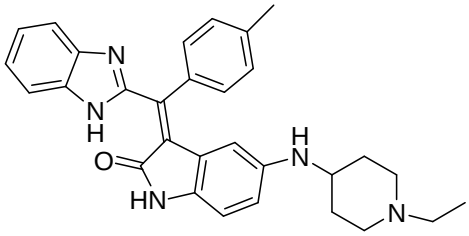	8	8.096

36*	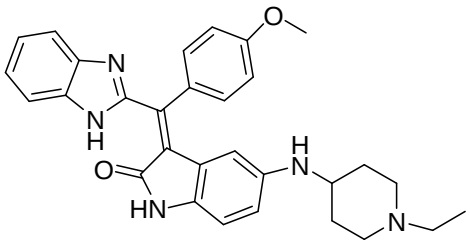	13	7.886
37*	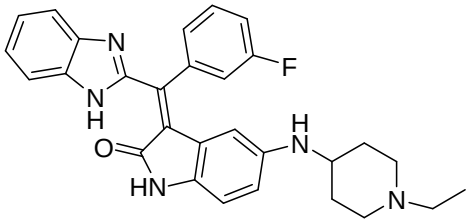	3	8.522
38*	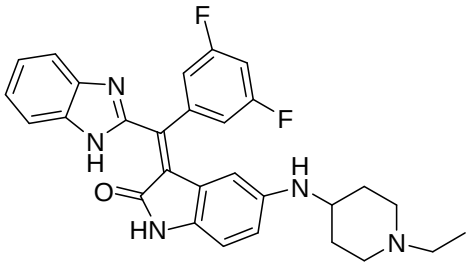	4	8.397
39	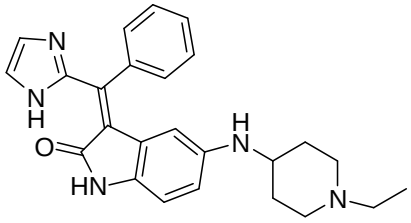	16	7.795
40	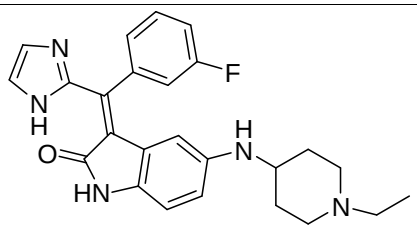	7	8.154
41	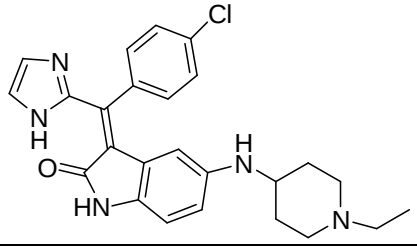	4	8.397
42	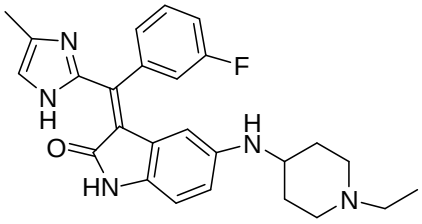	20	7.698

43	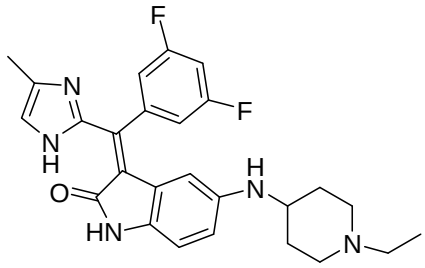	11	7.958
44	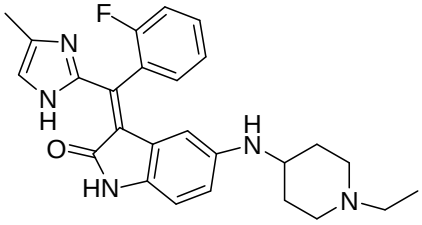	29	7.537

**indicate test set compound*

Figure 1. Fragment used as a common structure for aligning database for generation of CoMFA and CoMSIA models

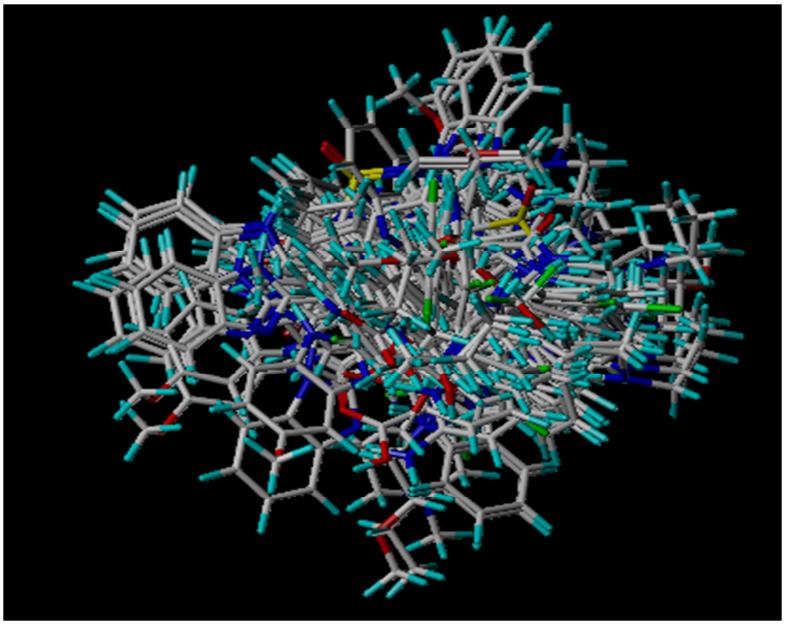

Figure 2. For CoMFA and CoMSIA study 1-44 aligned compounds

CoMFA and CoMSIA fields Generation

For each alignment, the steric and electrostatic potential fields for CoMFA were calculated at each lattice intersection of a regularly spaced grid of 2.0 Å in all X, Y and Z directions. The van der Waals potential and columbic term, which represent respectively, electrostatic and steric fields, were calculated by use of Tripos force field. A sp^3 carbon atom with van der Waals radius of 1.52 Å and +1.0 charges was served as the probe atom to calculate steric and electrostatic fields. The steric and electrostatic contributions were truncated to default ±30 kcal/mol, and the electrostatic contribution was ignored at lattice intersections with maximum steric interaction.

CoMSIA is an extension of CoMFA on the same assumption that changes in binding affinities of ligands are related to changes in molecular properties represented by the field. Besides, steric and electrostatic, hydrogen bond donor, hydrogen bond acceptor and hydrophobic descriptors are calculated in CoMSIA. A Gaussian function was introduced to determine the distance between probe atom and molecular atom at all grid point similarity indices at the molecular surface can be calculated in CoMSIA[23]. The equation for CoMSIA is as follow:

$$A^{q}_{F,K(j)} = \sum_i W_{probe,k}\, W_{ik} e^{-\alpha r^2_{iq}} \quad (1)$$

where, A is the similarity index at grid point q, summed over all atoms i of the molecule j under investigation. W_{probe}, k is the probe atom with radius 1 Å, charge +1, hydrophobicity +1, hydrogen bond donating +1 and hydrogen bond accepting +1. W_{ik} is the actual value of the physicochemical property k of atom i. r_{iq} is the mutual distance between the probe atom at grid point q and atom i of the test molecule. α is the attenuation factor whose optimal value is normally between 0.2 and 0.4, with a default value of 0.3 [24].

Partial least square analysis and model validation

For development of 3D-QSAR, CoMFA and CoMSIA studies were carried out using partial least square (PLS) approach which is an extension of multiple regression analysis [25-26]. All the data set of definite molecules was further treated by using PLS analysis technique and development of 3D contour maps with an optimum number of components 6 equally. PLS algorithm was used to develop the correlation between the structural property and biological activity. By use of PLS leave one out (LOO) and cross-validation analysis was performed. In cross-validation method one molecule is subtracted from the data set and its activity is predicted referencing the model obtain from rest of the data set. The cross-validation coefficient is represented as q^2. The models were accepted if model provides value of $q^2 > 0.5$ and $r^2 > 0.641$ [27]. It is generally estimated as:

$$q^2 = 1 - \frac{\sum \left(Y_{predicted} - Y_{observed}\right)}{\sum \left(Y_{observed} - Y_{mean}\right)} \quad (2)$$

While, the validation of conventional correlation co-efficient r^2, standard error of estimate (SEE) and F values were carried out in non-cross validation method. At the end bootstrap analysis was performed to check the robustness of the generated model, It is a method which carried out numerous times (for good statistical information 100 times required) in which n random selections are carried out from the original set of n object,. During every run, certain molecules can be omitted from the Partial Least Square analysis, while remaining molecule must be involved many times. Bootstrap r^2 (r^2_{bs}) represented mean correlation coefficient. For CoMFA and CoMSIA analysis cross-validation (r^2_{cv}) was carried out by two groups ('leave half out' method) [28].

Predictive correlation coefficient (r^2_{pred})

The test set of nine compounds was used to determine the predictive power of generated 3D-QSAR model. Template structure was used to align the compounds and their pIC_{50} values were predicted. Based on the test set compounds, the predictive correlation coefficient (r^2_{pred}) was determined by the following equation:

$$r^2_{pred} = \frac{(SD - PRESS)}{SD} \quad (3)$$

where, SD is the totality of squared deviation between biological activity of the test set compounds and mean activities of the training set compounds, and PRESS is the totality of squared deviations between experimental and predicted activity values for each compound in the test set [29].

RESULTS AND DISCUSSION

CoMFA studies

The training set and test set was utilized to develop CoMFA model. For model, Partial Least Square method was carried out with Leave One leave out which demonstrated the value of q^2 =0.758 through optimum 6 components. Column filtering 2.0 and same five components was utilized for Non cross-validated (r^2_{ncv}) PLS analysis, which gives r^2_{ncv} = 0.952, significance value *F* = 122.338, standard error of estimation (SEE) = 0.255 and predictive power r^2_{pred} of 0.885. A contribution of Steric and electrostatic fields were found to be 4.626 and 1.189, respectively. Results obtained throw CoMFA analysis is represented in Table 2. The Cross-validation and bootstrapping result strongly support reliability of the CoMFA model. The experimental and predicted pIC_{50} values for the training set and test set are shown in Table 4 and 5 respectively, and the experimental and predicted activities correlation in the form of scatter graphs are presented in Figures 3 and 4 respectively.

Table 2. Statistical parameter by using PLS analysis for CoMFA

PLS analysis parameter	*CoMFA*
r^2_{loo} (q^2)	0.758
ONC	6
SEE	0.255
r^2_{ncv}	0.952
F value	122.338
Steric field contribution	4.626
Electrostatic field contribution	1.189
r^2_{bs}	0.984
SEE_{bs}	0.154
r^2_{cv}	0.746
Test set r^2_{pred}	0.885

Table 3. Statistical parameter by using PLS analysis for CoMSIA

Sr. No.	Descriptors*	$r^2_{LOO}(q^2)$/ ONC	r^2_{ncv}/ SEE_{ncv}	F value	r^2_{cv}	r^2_{bs}/ SEE_{bs}
1	S and E	0.729/6	0.835/0.473	31.103	0.744	0.938/0.284
2	D and A	0.569/6	0.911/0.348	62.817	0.563	0.957/0.255
3	**S, E and H**	**0.805/6**	**0.934/0.299**	**87.329**	**0.714**	**0.971/0.196**
4	S, E and A	0.751/6	0.883/0.398	46.558	0.767	0.978/0.137
5	S, E and D	0.688/6	0.907/0.355	60.266	0.687	0952/0.240
6	D, A and H	0.737/6	0.945/0.273	106.04	0.737	0.971/0.200
7	D, A and S	0.648/6	0.920/0.330	70.656	0.641	0.952/0248
8	D, A and E	0.635/6	0.916/0337	67.223	0.642	0.950/0.254
9	S, D and H	0.643/6	0.940/0.285	96.400	0.592	0.979/0.164
10	S, E, D and A	0.666/6	0.916/0.201	67.365	0.665	0.963/0.223
11	S, E, D and H	0.750/6	0.929/0.311	80.397	0.770	0.963/0.217
12	S, E, A and H	0.782/6	0.931/0.307	82.615	0.737	0.961/0.220
13	D, A, H and S	0.711/6	0.943/0.278	101.97	0.755	0.975/0.194
14	D, A, H and E	0.722/6	0.943/0.278	101.58	0.761	0.969/0.201
15	S, E, D, A and H	0.731/6	0.937/0.293	91.130	0.725	0.967/0.215

CoMSIA studies

Same training set and test set was utilized for CoMSIA model development because, significant results were found with CoMFA. Steric, electrostatic, hydrophobic, hydrogen bond acceptor and hydrogen bond donor fields were used for generation of CoMSIA model with various combinations of these molecular descriptors as shown in Table 6. The statistical quality of hybrid models was examined by studying the corresponding q^2 values. The model–3 generated using descriptors steric, electrostatic and a hydrophobic field was found to be best CoMSIA model. So this model was further utilized for analysis. The cross-validation (q^2) value for corresponding CoMSIA model was obtained 0.805 by six optimum numbers of components (ONC). Column filtering 2.0 and Similar six components was utilized for non-cross-validated (r^2_{ncv}) PLS analysis, resulting in r^2_{ncv}= 0.934 and SEE = 0.299. The steric contribution = 1.113, electrostatic contribution = 1.498, hydrophobic contribution = 2.573 predictive power of CoMSIA r^2_{pred} was found to be 0.961. Leave half out cross-validation method and boot strapping analysis was performed to determine the quality of developed model. For the CoMSIA, $r^2_{cv}$was found to be 0.714. To analyze the internal reliability within the dataset the mean r^2value of bootstrapping analysis (bootstrapped r^2_{bs}) and SEE_{bs} were

performed which was found to be 0.971 and 0.196 respectively. Statistical parameter obtained throws CoMSIA model is represented in Table.3.

According to the CoMSIA model, experimental and predicted pIC_{50} values for training set and test set are represented in Table. 4 and 5 respectively while, the relationships between experimental and predicted inhibitory activities are represented in the form of scatter graphs in Figures 3 and 4 respectively.

Table 4. Experimental, predicted pIC_{50} and residual values of training set compounds by CoMFA and CoMSIA analysis

		CoMFA		*CoMSIA*	
Compound no.	*Experimental value*	*Predicted*	*Residual*	*Predicted*	*Residual*
2	6.924	6.436	0.488	6.653	0.271
3	7.055	6.725	0.330	6.838	0.217
5	6.903	6.967	-0.064	6.929	-0.026
6	6.974	6.826	0.148	6.566	0.408
7	6.537	6.232	0.305	6.164	0.373
10	6.485	6.495	-0.009	6.548	-0.062
12	7.167	6.936	0.231	6.726	0.441
13	7.292	6.846	0.446	6.608	0.684
14	5.311	6.099	-0.787	7.051	-1.739
15	5.311	5.404	-0.092	5.605	-0.293
16	8.397	8.709	-0.311	8.365	0.032
17	6.670	6.361	0.310	5.841	0.830
18	4.626	5.045	-0.418	5.281	-0.654
19	7.494	7.771	-0.276	7.428	0.066
20	8.301	8.404	-0.103	8.446	-0.145
21	7.086	7.184	-0.098	7.656	-0.570
23	7.221	7.308	-0.086	7.436	-0.214
24	7.823	7.785	0.038	7.368	0.455
25	7.161	7.552	-0.390	7.250	-0.088
26	6.804	6.919	-0.119	7.032	-0.227
29	5.709	5.576	0.133	5.578	0.131
31	6.560	6.431	0.129	7.276	-0.715
32	8.000	8.074	-0.074	7.444	0.556
33	8.090	8.165	-0.075	8.272	-0.182
35	8.096	8.035	0.061	7.916	0.180
39	7.795	7.968	-0.172	8.026	-0.230
40	8.154	8.242	-0.0871	8.362	-0.207
41	8.397	8.312	0.085	7.794	0.603
42	7.698	7.706	-0.0071	7.735	-0.036
43	7.958	7.814	0.144	7.746	0.212
44	7.537	7.523	0.014	7.449	0.088

Table 5. Experimental, predicted pIC_{50} values and residual values of test set compound by CoMFA and CoMSIA analysis

		CoMFA		*CoMSIA*	
Compound no.	*Experimental value*	*Predicted*	*Residual*	*Predicted*	*Residual*
1	7.013	6.818	-0.804	7.000	0.132
4	6.198	6.250	-0.051	6.525	-0.051
8	4.701	5.004	-0.300	4.936	-0.235
9	5.661	5.300	0.361	5.184	0.477
11	5.005	5.143	-0.138	5.272	-0.267
22	8.522	8.475	0.047	8.008	0.514
27	5.945	5.961	-0.015	6.205	-0.259
28	6.180	6.261	-0.081	6.244	-0.063
30	7.657	7.773	-0.115	7.839	-0.181
34	8.221	8.164	0.057	8.000	0.221
36	7.880	7.74	0.146	7.964	-0.078
37	8.522	8.414	0.108	8.537	-0.014
38	8.397	8.313	0.08	8.363	0.034

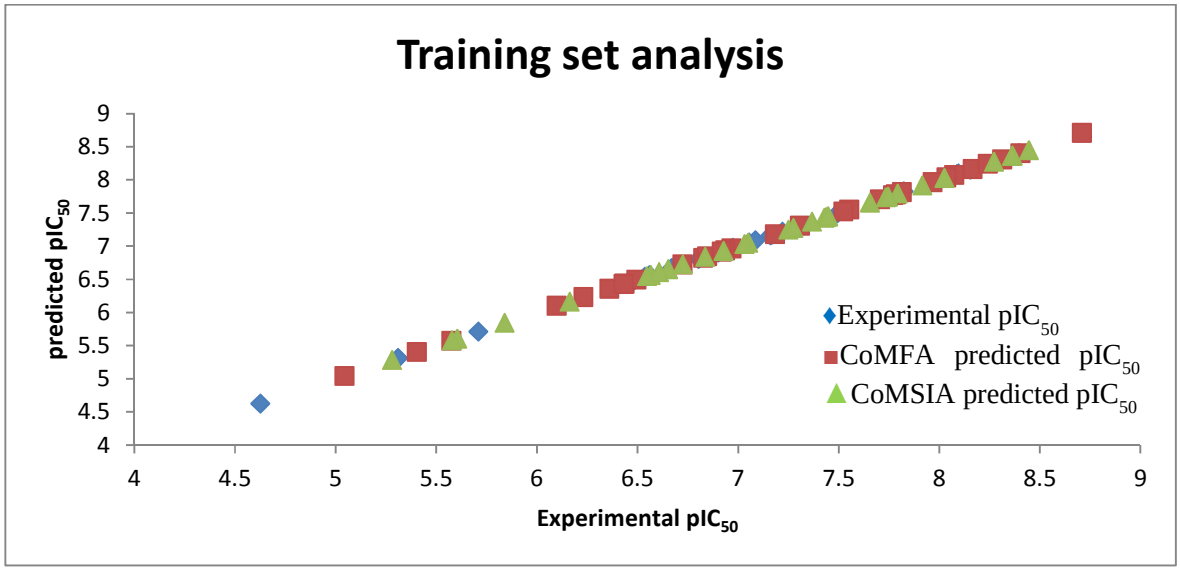

Figure 3. Graph of actual and predicted pIC_{50} value for training set by CoMFA and CoMSIA analysis

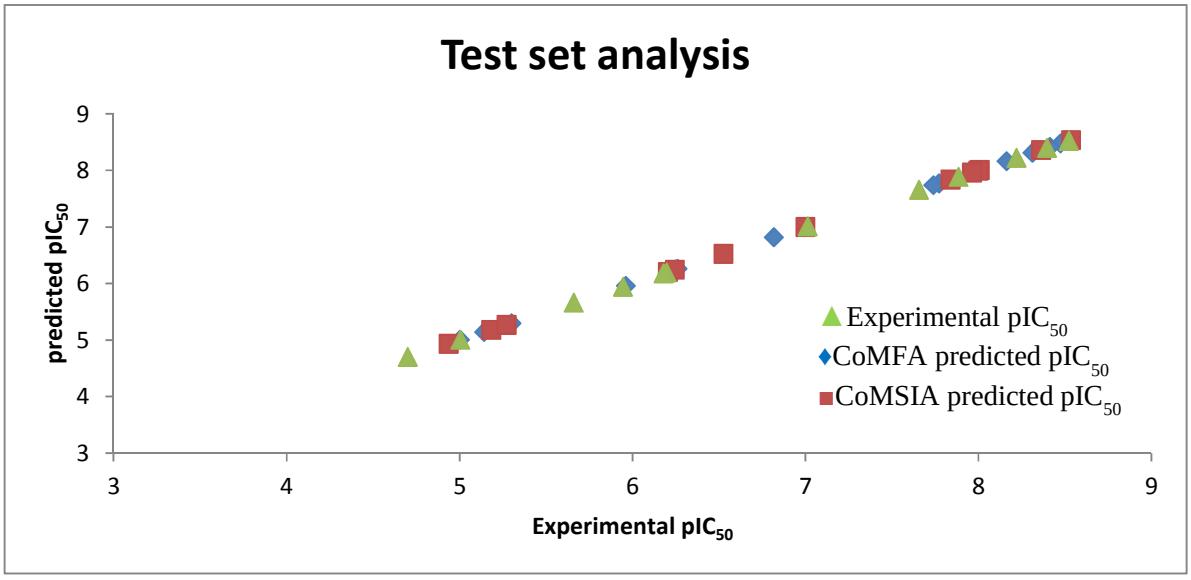

Figure 4. Graph of actual and predicted pIC_{50} value for test set by CoMFA and CoMSIA analysis

3D-QSAR visualization

CoMFA

The significant feature of CoMFA model is the outcomes obtained by 3D coefficient contour maps which are calculated as the variation in the molecular fields multiplied by the 3D-QSAR coefficient by using Model stDev*Coeff. CoMFA contour maps were generated to identify the important regions in 3D space surrounding the molecules, so that modification can be carried out in those areas to increase the inhibitory activity, which may be utilized to improve VEGFR-2 inhibitory activity.

The most active compound 44 and least active compound 18 were used to generate contour maps by managing style of contour to transparent for better analysis of contour surrounding compound 44 which represented in Figures 6 (a, b) and for compound 18 represented in Figure 6 (c, d) includes steric and electrostatic region respectively. The steric region signs two colours in contour maps i.e. green and yellow. In which green color indicates the favourable part, keeping the bulkier group which leads to an increase in the biological activity whereas; yellow color indicates a

decrease in the biological activity due to the bulkier region. Further, the electrostatic contour map shows red and blue color. The red color and blue color indicates the favourable and unfavourable region respectively. Here, red color region indicate that biological activity enhanced by negative charge while, blue color region indicates positive charge leads to increase in biological activity.

CoMSIA

CoMSIA contour maps were generated similarly as contour maps generated by CoMFA. For the CoMSIA total 5 contour maps were generated; for steric, electrostatic, hydrophobic, donor and acceptor fields. The steric and electrostatic region has the same description like CoMFA. Whereas; the hydrophobic has yellow and white color codes in which yellow color indicate hydrophobic group favorable; while white color indicates hydrophobic group unfavorable. The donor has cyan and purple color; cyan color indicates donor group favorable; while purple indicates acceptor group favorable. They show which part/substitute can help to find out the favorable and unfavorable region.

Analysis of CoMFA and CoMSIA contour map

CoMFA

Figure 6 (a, c) depicts the CoMFA steric contour plot. Whereas, Figure 5 represents most active compound 44 is divided into three major regions (**A**, **B** and **C**). A large cloud of green contour found surrounding **C** region at oxiindole ring indicates that the introduction of a bulky group in this region is favored which explains the importance of steric interaction of ligand with receptor.

Similarly, green contour near **B** region at phenyl ring indicate that bulky group is favored at this region. This is evident from the experimental activity values for compounds 34-44 in which at both region**B** and **C** large bulky group, than other compound 1-34 leads to potent VEGFR-2 inhibitory activity.

A yellow contour at **A** region in imidazole ring at C-3 position indicate the bulky group is not favored at this region which leads to decrease in activity. While at **C** region in oxiindole ring very large bulky group leads to decrease in activity.

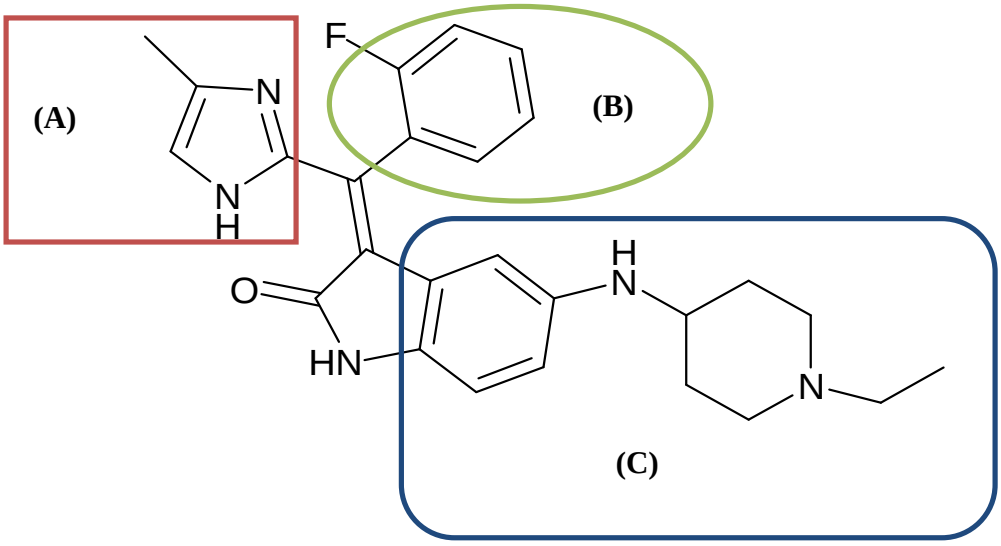

Figure 5. Most potent compound 44 divided into (A), (B) and (C) regions

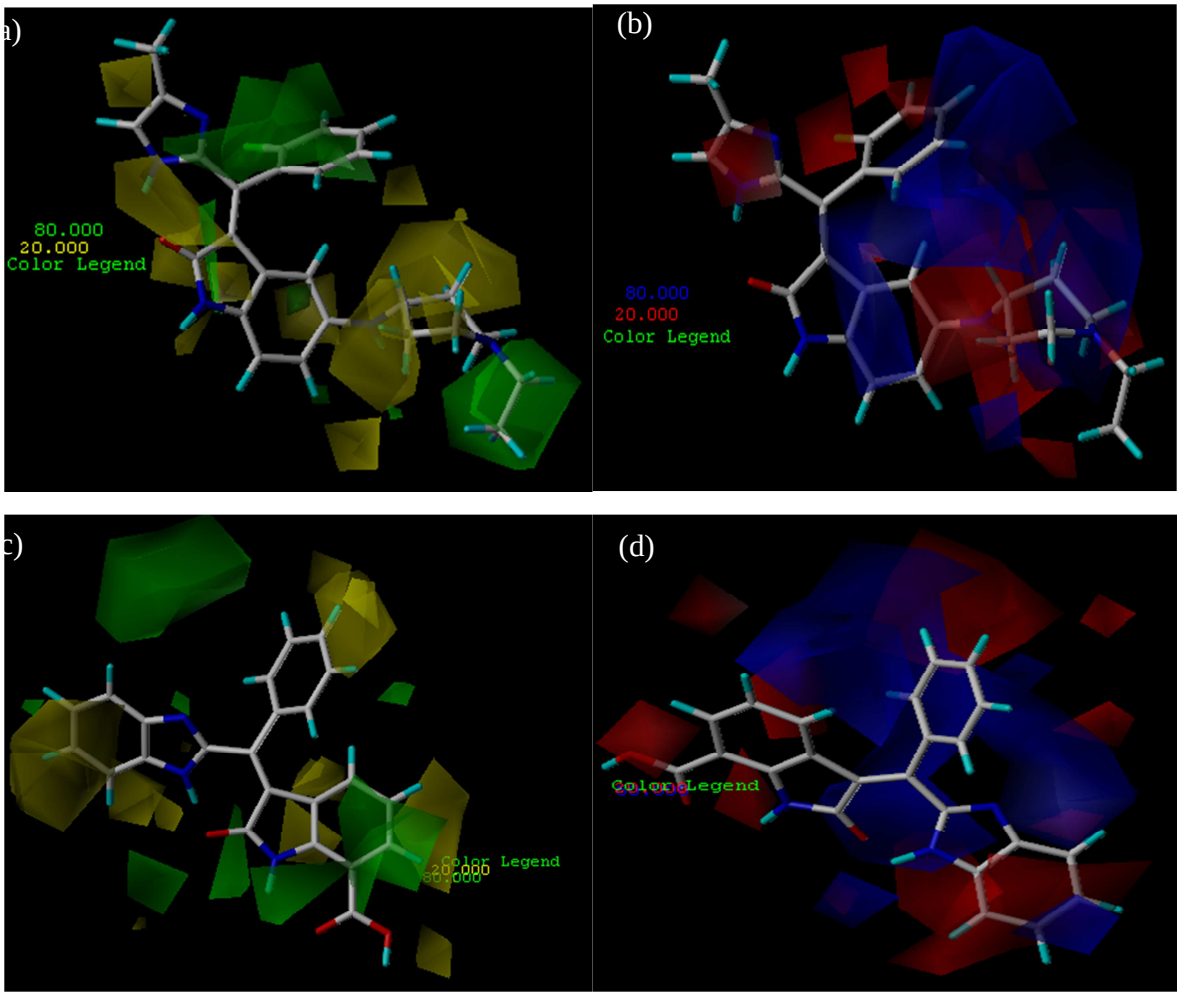

Figure 6. Steric contour maps (a, c) and electrostatic contour maps (b, d) generated by comparative molecular field analysis (CoMFA) for the most active compound 44 (a, b) and the less active compound 18 (c, d), respectively

Figure 6(b, d) displays the electrostatic contour map using CoMFA. The electrostatic fields are represented by blue and red contour map. Compound 44 was again selected as the reference standard as seen in figure 6b, blue contour near **B** and **C** region indicates that need for positively charged substituent for electrostatic interaction with the receptor to show potent inhibitory activity. While, red contour at **A** region at imidazole ring indicates that introduction of negatively charged group leads to increase in the biological activity.

CoMSIA

Contour map for steric and electrostatic fields in CoMSIA models are almost the same as those in the CoMSIA model. Few more contours are seen for the steric and electrostatic fields which are elaborated here. The yellow contour seen at **B** region near the carbonyl group in oxiindole ring shows that the large bulky group is not favored in this region for better activity.While, green contour at phenyl ring in **B** region and **C** region suggest that presence of large bulky group leads to increase in inhibitory activity.

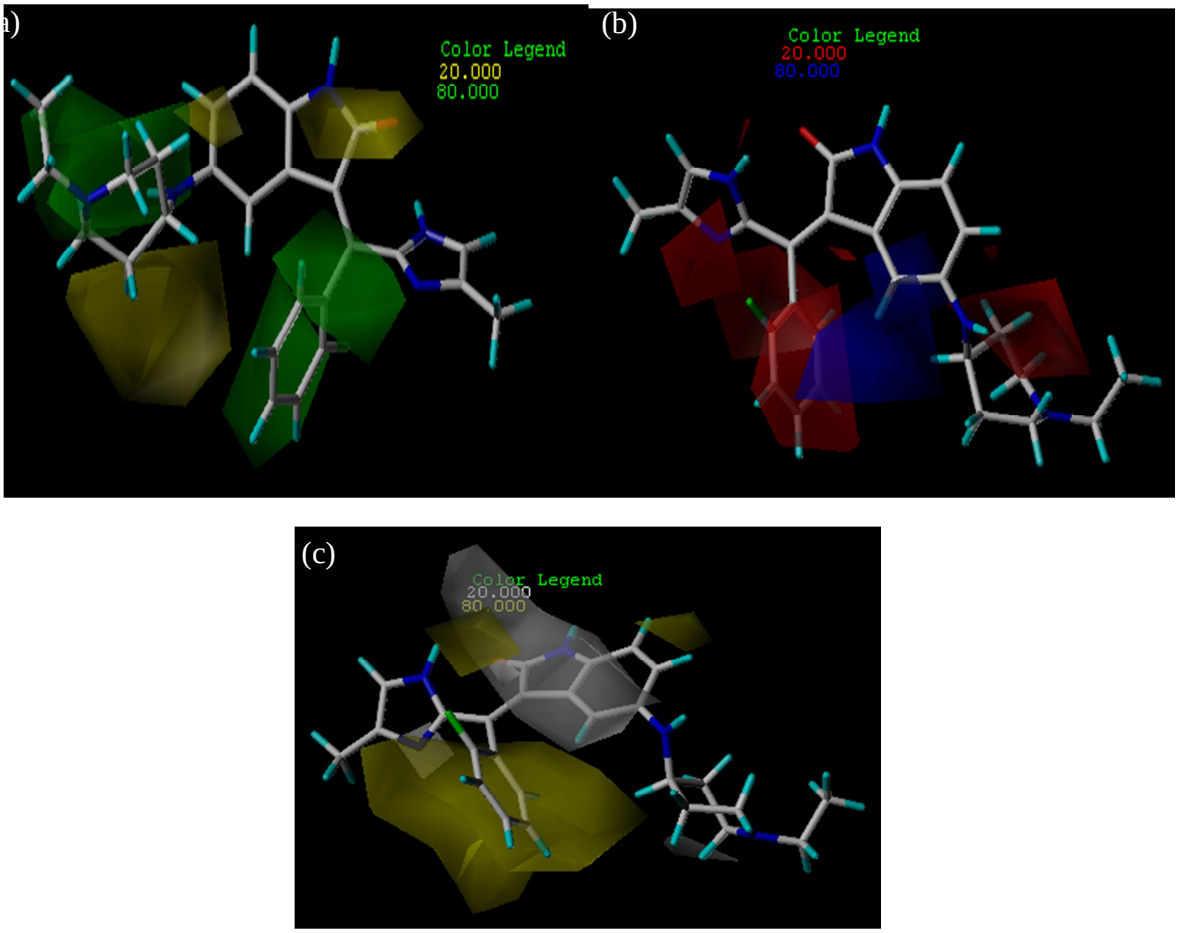

Figure 7. Comparative molecular similarity indices analysis (CoMSIA) for most active compound 44 (a) Steric map (green, bulky group desirable; yellow, bulky group not desirable), (b) electrostatic map contour map (blue, electropositive group desirable; red, electronegative group desirable), (c) hydrophobic map (yellow, hydrophobic group desirable; white, hydrophilic group desirable)

In Figure 7b, the red contour in phenyl ring at **B** region indicating that replacement of hydrogen atoms with negatively charged atoms leads to increase in the activity. This is evident from experimental activity of compounds 37-44 in which negatively charged group present leads to potent inhibitory activity. While at **B** region in oxiindole ring introduction of positively charged substituents leads to increase in activity.

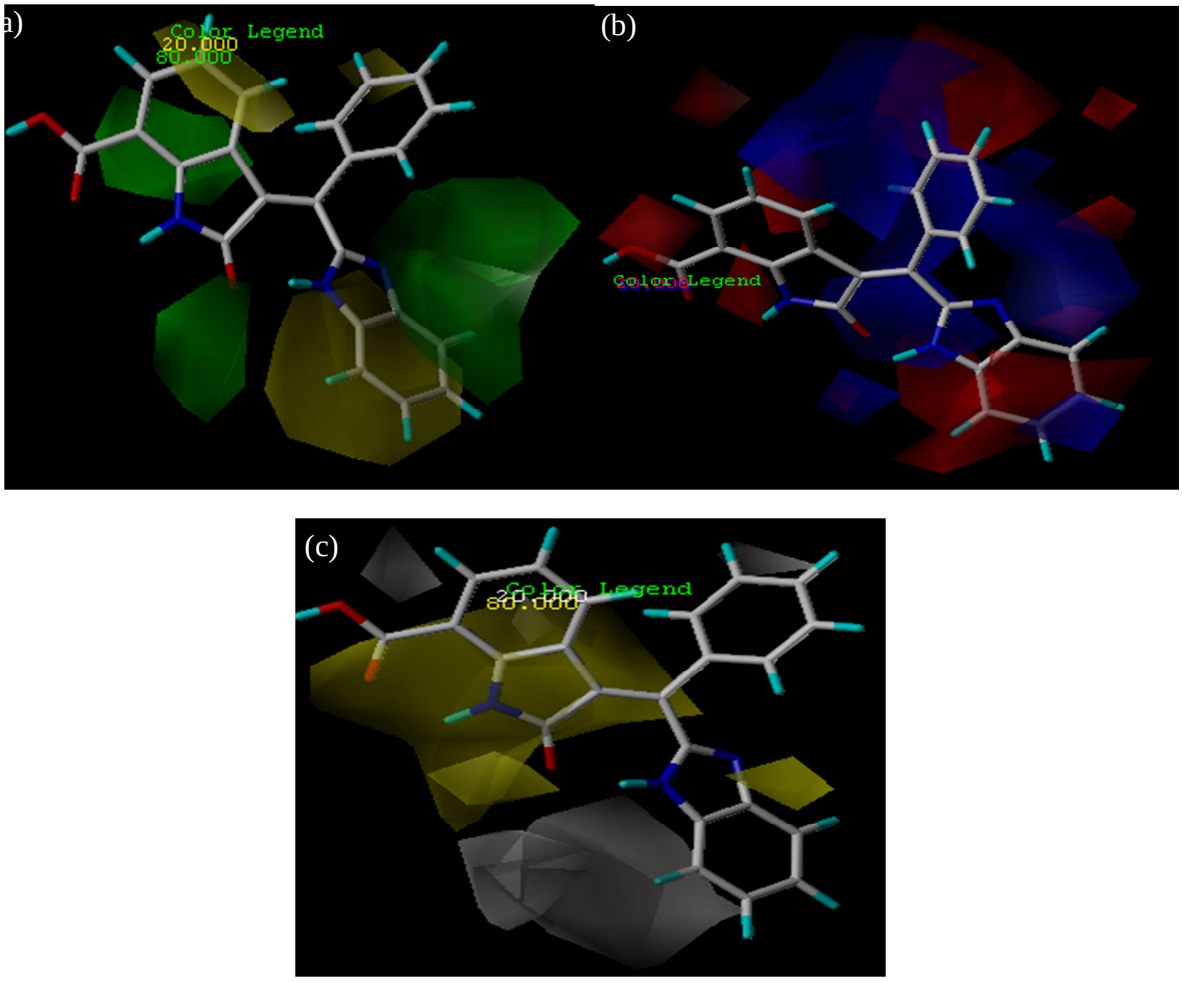

Figure 8. Comparative molecular similarity indices analysis (CoMSIA) for least active compound 18 (a) Steric map (green, bulky group desirable; yellow, bulky group not desirable), (b) electrostatic map contour map (blue, electropositive group desirable; red, electronegative group desirable), (c) hydrophobic map (yellow, hydrophobic group desirable; white, hydrophilic group desirable)

The yellow region in CoMSIA hydrophobic contour plot indicates that hydrophobic substituent in this region enhance inhibitory activity while white contour map indicates that hydrophilic substituent will improve activity. In figure 7c, the yellow contours for compound 44 observed in **B** region at phenyl ring indicate bulky and hydrophobic substituent are favorable in this region.

While, in **C** region white contour map indicates that hydrophilic substituent are favored in this region. This is evident from experimental activity values for compound 34 to 44 in which hydrophobic substituent at phenyl ring which shows potent inhibitory activity.

CONCLUSION

In the present study, CoMFA and CoMSIA are performed using set of vascular endothelial growth factor receptor inhibitors. Partial Least Square (PLS) analysis was performed in order to correlate the CoMFA and CoMSIA descriptors with the observed experimental inhibitory activity. A significant 3D-QSAR model was generated. This model was further validated by various statistical parameters and all were found to be significant with excellent predictability. The model obtained from CoMFA and CoMSIA have the values of q^2=0.758, r^2_{ncv}=0.952, ONC= 6; q^2=0.805, r^2_{ncv}=0.934, ONC=6 respectively. The predictive power of the model was validated by using test set of nine 13 compound and was found to be the values of r^2_{pred}as 0.885and 0.861 of CoMFA and CoMSIA respectively. To check the robustness and statistical confidence of the derived models, the boot-strapping analysis was performed.

From the contour map study from each model it was observed that bulky group is favored at B and C region in phenyl ring and oxiindole ring respectively. But not at **A** region. Similarly negatively charged substituent at phenyl ring in B region leads to potent inhibitory activity. Hence the CoMFA and CoMSIA models can be used further to design novel indolin derivatives as the potent vascular endothelial growth factor receptor inhibitor for treatment of cancer.

Acknowledgements
The authors are grateful to Dr. Shivajirao S. Kadam, Vice Chancellor, Bharati Vidyapeeth University, Pune, Maharashtra, India.

REFERENCES

[1] G. Atalay, F. Cardoso, A. Awada, M.J. Piccart, *Annals of Oncology*., **2003,14**, 1346–1363.
[2] I.W. Tremont-Lukats, M.R. Gilbert, *Cancer Control*., **2003,10,125**–137.
[3] T. V Petrova, T. Makinen, K. Alitalo, *Experimental Cell Research*., **1999**, 253,117–130.
[4] T. Matsumoto, H. Mugishima, *Journal of Atherosclerosis and Thrombosis*.,**2006**,13,130–135.
[5] S. Kanno, N. Oda, M. Abe, Y. Terai, M. Ito, K. Shitara, et al., *Oncogene*.,**2000**,19,2138–2146.
[6] Y. Sato, S. Kanno, N. Oda, M. Abe, M. Ito, K. Shitara, et al., *Annals of the New York Academy of Sciences*.,**2000**, 902, 201–207.
[7] A. Gauthier, M. Ho, *HepatologyResearch*.,**2013**, 43,147–154.
[8] R.J. Motzer, T.E. Hutson, P. Tomczak, M.D. Michaelson, R.M. Bukowski, O. Rixe, et al., *New England Journal of Medicine*.,**2007**, 356, 115–124.
[9] M. Gross-Goupil, L. François, A. Quivy, A. Ravaud, *Oncology*.,**2013**,7,269.
[10] N. Degrauwe, J.A. Sosa, S. Roman, H.A. Deshpande, *Clinical Medicine Insights Oncology*.,**2012**,6, 243.
[11] W.T.A. van der Graaf, J.-Y.Blay, S.P. Chawla, D.-W. Kim, B. Bui-Nguyen, P.G. Casali, et al., *The Lancet*.,**2012**, 379, 1879–1886.
[12] M.H. Kim, A.L. Tsuhako, E.W. Co, D.T. Aftab, F. Bentzien, J. Chen, et al., *Bioorganic & Medicinal Chemistry Letters*.,**2012**,22,4979–4985.
[13] J. Verma, V.M. Khedkar, E.C. Coutinho, *Current Topics in Medicinal Chemistry*.,**2010**,10, 95–115.
[14] G. Klebe, U. Abraham, T. Mietzner, *Journal of Medicinal Chemistry*.,**1994**, 37, 4130–4146.
[15] R.D. Cramer, *Journal of Medicinal Chemistry*.,**2003**, 46 ,374–388.
[16] S. Shinkaruk, M. Bayle, G. Lain, G. Deleris, *Current Medicinal Chemistry-Anti-Cancer Agents*.,**2003**, 3, 95–117.
[17] A. Balupuri, P.K. Balasubramanian, S.J. Cho, *Archives of Pharmacal Research*., **2015**, 38, 1434–1442.
[18] D.C. Juvale, V. V Kulkarni, H.S. Deokar, N.K. Wagh, S.B. Padhye, V.M. Kulkarni, *Organic &Biomolecular Chemistry*.,**2006**, 4 , 2858–2868.
[19] A. V Raichurkar, V.M. Kulkarni, *Journal of Medicinal Chemistry*.,**2003**, 46,4419–4427.
[20] X. Li, M. Shu, Y. Wang, R. Yu, S. Yao, Z. Lin, *Current Computer-Aided Drug Design*.,**2014**, 10,327–334.
[21] P.S. Kharkar, B. Desai, H. Gaveria, B. Varu, R. Loriya, Y. Naliapara, et al., *Journal of Medicinal Chemistry*.,**2002**, 45,4858–4867.
[22] SYBYL-X **2012**. Molecular Modeling Software, Tripos Associates Inc, V. 2.0, St. Louis, USA.
[23] J. Zheng, G. Xiao, J. Guo, Y. Zheng, H. Gao, S. Zhao, et al., *Chemical Biology & Drug Design*., **2011**,78, 314–321.
[24] M. Böhm, J. Stürzebecher., G. Klebe, *Journal of Medicinal Chemistry*.,**1999**, 42, 458–477.
[25] J.K. Buolamwini, H. Assefa, *Journal of Medicinal Chemistry*.,**2002**, 45, 841–852.
[26] S. Li, R. Zhang, H. Du, *Journal of Chemistry*.,**2013**.
[27] A. Golbraikh, A. Tropsha,,*Journal of Molecular Graphics and Modelling*., **2002**, 20, 269–276.
[28] S.G. Bhansali, V.M. Kulkarni., *SAR and QSAR in Environmental Research*.,**2014**, 25, 905–937.
[29] G.-W. Rao, C.-H.Hu, J.-B.Ni, J. Wang, C. Wang, B.-L. Wang, *Medicinal Chemistry Research*.,**2014**, 23, 3244–3254.